GEOPHYSICAL RESEARCH LETTERS, VOL. 25, NO. 22, PAGES 4229-4232, NOVEMBER 15, 1998

Mapping the Moho beneath the southern Urals with wide-angle reflections

R. Carbonell[1], D. Lecerf [2], M. Itzin[2], J. Gallart[1], D. Brown[1]

Abstract. A stack of the wide-angle reflection/refraction component of the URSEIS-95 experiment provides the first well-resolved imaged of the Moho beneath the southern Urals. The processing consisted of low pass filter (0 - 6 Hz), CMP sorting, and a NMO correction without stretch. The PmP phase, a very narrow band and low frequency (up to 6 Hz) wavelet, changes character from west to east along the transect. In the depth converted section, the Moho reaches a maximum depth of 53 ± 2 km beneath the Magnitogorsk arc. Thickness estimates determined from high amplitudes at near critical distances also support a 53 km thick crust. A selective offset stack consisting of traces at 150 - 250 km offset indicate an undulating, irregular Moho, suggesting either strong lateral velocity variations or high topographic relief beneath the Magnitogorsk arc.

Introduction

The presence of a crustal root beneath an old orogenic belt is an intriguing and fundamental aspect of its post-orogenic evolution. Although an orogenic root has been reported from an older orogen (Trans-Hudsonian [Hajnal et al., 1996]), the Urals is thought to be unique among Paleozoic orogens such as the Appalachians, Variscides, and Caledonides in that it appears to have a crustal root along the central axis of the orogen that has been interpreted to extend to depths of 55 - 60 km (e.g., Druzhinin et al., et al., 1992, Berzin et al., 1996; Carbonell et al., 1996). Until now, however, none of the published geophysical data sets have provided a well resolved image of the Moho beneath the southern part of the Urals.

The URSEIS-95 experiment [Berzin et al., 1996] acquired deep seismic reflection and refraction data across the entire southern Urals [Echtler et al., 1996; Knapp et al., 1996], imaging the internal architecture of the orogen, but was unable to resolve the Moho along the orogenic axis, beneath the volcanic arcs. By forward modelling of identified PmP arrivals in the refraction/wide angle component of URSEIS-95 from four shot points (Fig. 1), Carbonell et al. [1996] established a maximum Moho depth of 55 - 58 km, but were unable to provide a continuous Moho image. To the north, in the central Urals, the ESRU deep seismic reflection experiment across the western and central part of the orogen [e.g., Juhlin, et al., 1996] images the Moho beneath the Tagil volcanic arc as a decrease in reflectivity at ~15 s TWT (~50 km). This correlates with the velocity models derived from the nearby GRANIT refraction profile [Juhlin et al., 1996]. The wide-angle seismic reflection fan shooting experiment UWARS [Thouvenot et. al, 1995] also indicates a maximum crustal thickness of ~55 km in the central Urals.

This paper presents the first well-resolved image of the Moho beneath the southern Urals using the URSEIS-95 wide-angle/refraction data set. The image, coupled with the travel time interpretation of the PmP phase and the CMP images of the normal incidence data sets provide a reasonable estimate of the increase in crustal thickness beneath the Magnitogorsk volcanic arc, and documents genetic differences in the Moho across the southern Urals.

Tectonic Setting and Crustal Structure

The southern part of the Uralide orogen (Fig. 1) formed as a result of subduction of the former East European Craton (EEC) eastward beneath the Magnitogorsk volcanic arc during the Late Devonian - Early Carboniferous, followed by closure of the paleo-Uralide ocean and accretion of terranes to the east along a west-dipping subduction zone from the Late Carboniferous to Early Triassic [e.g., Khain, 1985; Zonenshain et al., 1984, 1990; Brown et al., 1997, 1998; Puchkov, 1997]. From west to the east the southern Urals consists of a west-vergent thrust stack of EEC-derived Archean through Paleozoic rocks, structurally overlain by an allochthonous accretionary complex related to the arc-continent collision [Brown et al., 1997, 1998]. The former EEC is sutured to the Magnitogorsk arc along the Main Uralian fault (MUF), a wide, serpentinitic melange zone imaged on reflection seismic profiles as a zone of east-dipping weak reflectivity that can be traced to middle crust [Echtler et al., 1996, Brown et al., 1998]. The Magnitogorsk arc consists of Ordovician to Late Devonian volcanic and volcaniclastic rocks unconformably overlain by Carboniferous-age shallow water carbonates. East of the Magnitogorsk arc, the East Uralian zone consists of strongly deformed, imbricated and metamorphosed Precambrian and Paleozoic rocks of both continental and oceanic affinity [Puchkov, 1997]. This entire complex was heavily intruded by granitic rocks during the Late Devonian to Permian [Fershtater et al., 1997]. The East Uralian zone is bound to the east by the Troisk fault. The Trans Uralian zone, to the east of the Troisk fault, is poorly exposed and therefore not well known. It appears to consists predominantly of Paleozoic-age volcano-plutonic complexes that have been moderately deformed [Puchkov, 1997].

The crustal structure of the southern Urals is relatively well known from a number of Russian and recent deep seismic experiments including the URSEIS-95. The URSEIS-95 near vertical, CMP explosion and vibroseis data (Fig. 3c) show the southern Urals to be a bivergent collisional orogen that has apparently maintained its collisional seismic reflection architecture, suggesting it has been unaffected by post-orogenic collapse [Echtler et al., 1996, Knapp et al., 1996]. Reflectivity throughout the crust varies laterally, and correlates with the major tectonic units. The MUF is poorly imaged, being marked in the upper 3 - 4 s by some westward dipping reflections in a zone marking a change in reflectivity between the volcanic arc and the Precambrian basement. The boundary between the East Uralian and the Trans Uralian zones is imaged as a thick west dipping reflective package called the Kartaly reflection sequence (KRS) (Fig. 3c) [Echtler et al, 1996], that can be traced from the upper crust westward into the lower crust, where it appears to merge with the Moho. The Magnitogorsk arc is, however, only moderately reflective at upper crustal levels where discontinuous reflections occur, and the middle and

[1]Dept. Geophysics, Inst. of Earth Sciences, CSIC-Barcelona, Spain
[2]Geophysical Inst., Karlsruhe University, Karlsruhe, Germany

Paper number 1998GL900107.
0094-8276/98/1998GL900107$05.00

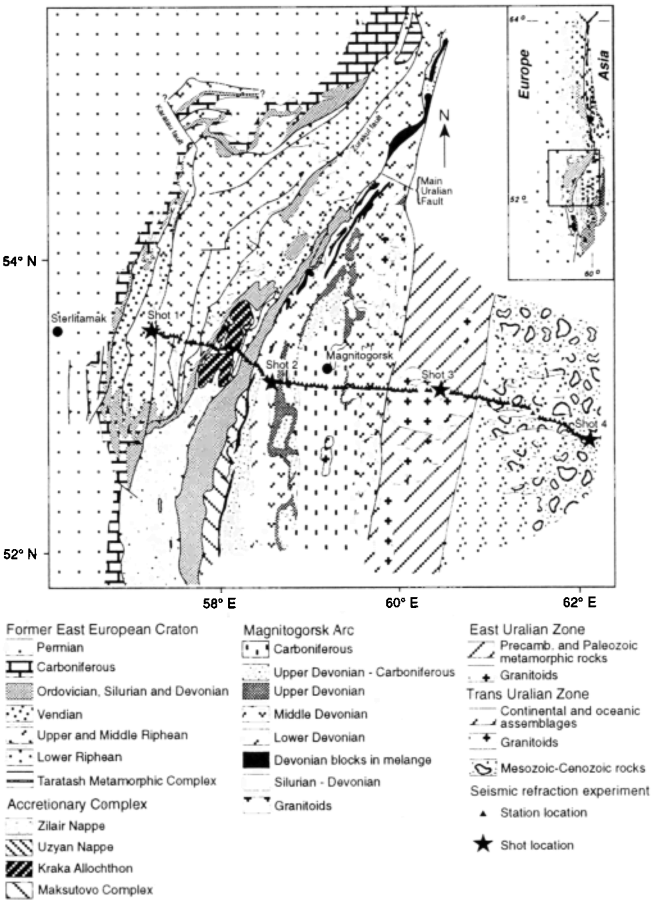

Fig. 1. Geologic sketch map indicating the major geologic units and tectonic structures of the southern Urals and showing the location of the URSEIS'95 wide-angle/refraction experiment with the station distribution and shot record locations are also marked.

lower crustal levels display only diffuse reflectivity. The reflection Moho is well defined only in the eastern and westernmost parts of the URSEIS-95 profile [Knapp et al., 1996], where it deepens toward the orogenic axis. The URSEIS-95 explosion source data has also revealed a number of enigmatic reflections within the mantle [Knapp et al., 1996; Steer et al., 1998].

Data Processing

A preliminary interpretation of the seismic refraction/wide-angle reflection data consisted of forward modelling of the travel time picks of the most prominent arrivals [Carbonell et al., 1996]. The principal aim here is to produce a well constrained image of the Moho using the URSEIS-95 refraction/wide-angle data. The processing steps used are; 1) increase the signal-to-noise ratio of the PmP arrival (band pass filtering), 2) apply a hyperbolic constant moveout function (comparable to the Normal Moveout (NMO) correction of CMP data) to flatten the Moho reflection, 3) build the CMP geometry, 4) produce a composite low fold wide angle stack. Well resolved images of the Moho using seismic refraction data have been obtained for the Alps [Valasek et al., 1991; 1997] with a similar scheme.

A detailed frequency analysis of the PmP arrival by spectral analysis and filter panels revealed that it was characterized by very low frequencies (up to 6 Hz). A low pass filter (0 - 4.6 Hz) produced an outstanding improvement in the image of the PmP phase.

Conventional NMO corrections applied to wide-angle seismic data results in stretching of the first arrivals that mask the images, so a NMO correction without stretch is favourable for stack processing of wide-angle shot gathers. To estimate the time shift from the travel time curve for a horizontal reflector, we use the equation of the hyperbola (equation 1):

$$t_x = (t_0^2 + x^2/\upsilon^2)^{1/2} \quad (1)$$

where t_0 is the time for offset x=0.0 km; x is the offset of the trace; and υ is an average velocity for the crust above the reflector.

$$\Delta t_x = t_x - t_0 \quad (2)$$

Equation (2) estimates the time shift Δt_x that has to be applied to a trace recorded at an offset of x to flatten a reflector that arrives at 0 km offset at a time t_0.

Both t_0 and the υ have some degree of freedom, but for the Moho in the Urals we have reasonable estimates for t_0 of 14 - 16 s and for υ_0 of 6.4 - 6.8 km/s (Thouvenot et al., 1995; and Carbonell et al., 1996). The CMP stacked section achieved using the moveout correction is equivalent to the CMP processing sequence, and conventional post-stack processing algorithms can be used. A depth section for the Urals can now be obtained by depth converting with υ = 6.6 km/s.

The amplitude pattern of the PmP phase observed at near critical distances can be used to further constrain the crustal root using the location of the critical reflection. The amplitudes recorded by the different instruments are a direct function of the gain, so each trace must be scaled appropriately to recover the

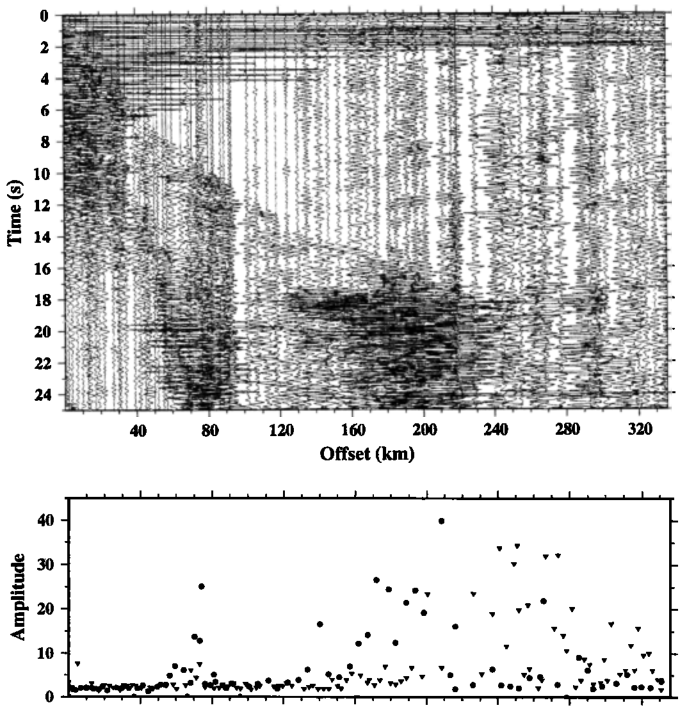

Fig. 2 Shot 1 with a hyperbolic moveout (Equation 1) and trace balanced by the RMS value of the amplitudes within a window around the PmP arrival (14 - 16 s). This image displays the prominent high amplitude anomaly at near critical distances of 150 - 160 km. B) Amplitude variation for the PmP phase for shot 1 (solid circles) and shot 4 (inverted, solid triangles). The high amplitude at approximately 70 km corresponds to the direct shear wave imaged Fig. 2a. The high amplitude anomaly at 150 - 160 km offset corresponds to the increase in amplitude of ther PmP phase at critical distances.

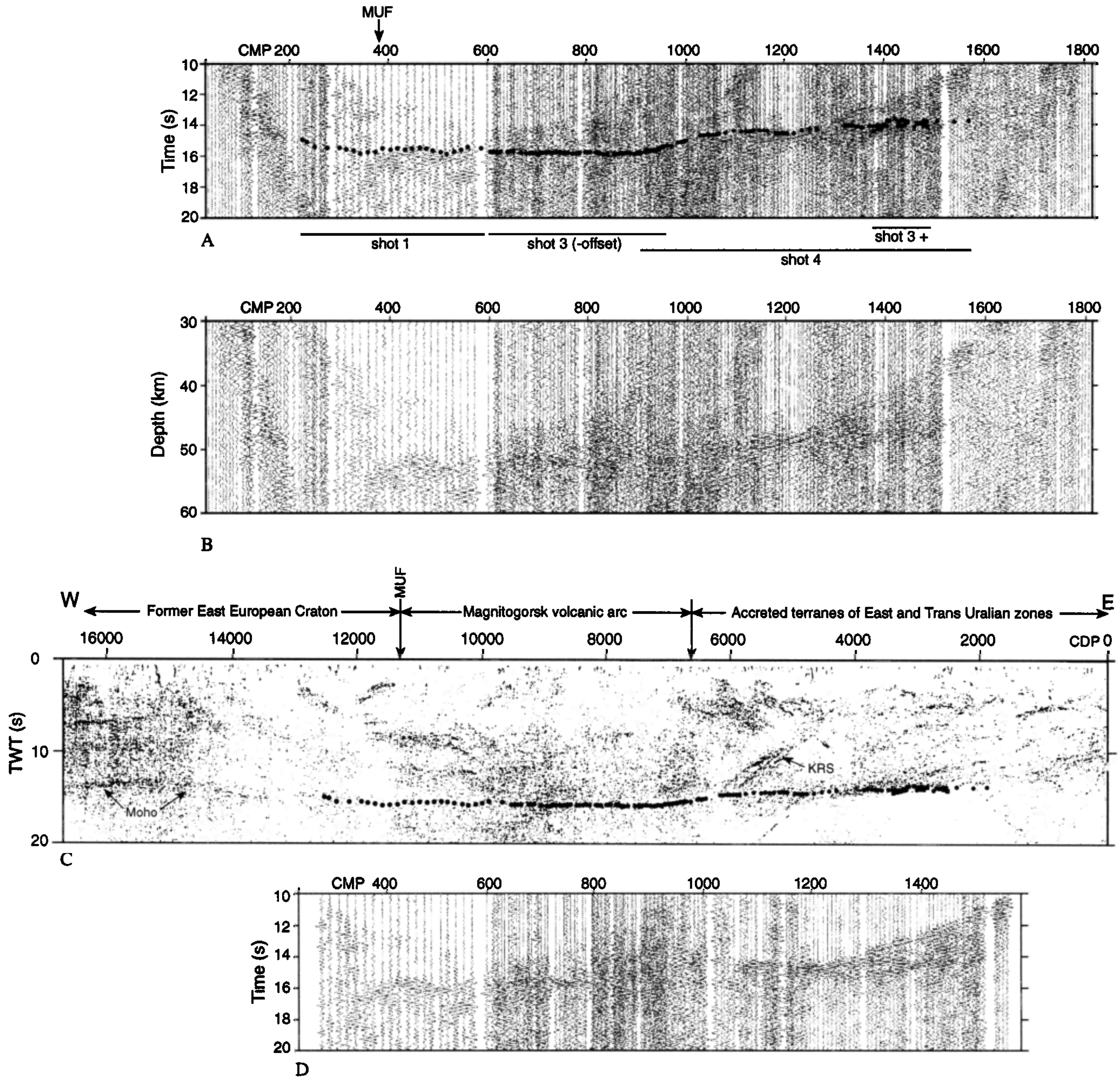

Fig. 3 A) Wide angle CMP stacked image obtained using the processing steps given in the text. B) Depth converted stack of Fig. 2a for a velocity of 6.6 km/s. C) URSEIS-95 stacked section of the explosive source data (from Steer et al. [1998]) with the wide angle Moho superimposed on it to illustrated the position of the Moho beneath the Magnitogorsk arc. D) A critical offset (100 - 250 km) low frequency image of the Moho beneath the Magnitogorsk arc.

correct amplitudes needed to determine critical distances (Fig. 2a). The correct amplitudes can be recovered by assuming that the background noise in all the instruments is the same and then scaling the traces using a background noise estimation. The background noise can be estimated by either calculating the root mean square (RMS) or the median value within a time window. The amplitudes within the window around the PmP arrival are equalized so that the RMS or Median values are constant from trace to trace. This trace balancing step can also increase the lateral continuity of reflections. The relatively large trace spacing (1 - 2.5 km) imposed by the experiment logistics and the lateral variability of the PmP phase poses additional difficulties for reliable phase correlations. To increase the lateral correlation and to determine amplitude anomalies at near critical distances for PmP arrivals, both the RMS and Median schemes were tested, and give similar results.

Discussion and Conclusion

A first estimate of the crustal thickness beneath the Magnitogorsk arc is obtained from the amplitude patterns at near critical distances. Shot's # 1 and # 4 display high amplitude PmP patterns that start near 150 km offset (Fig. 2b). The high amplitudes near 70 km offset corresponds to the shear wave direct arrival (Fig. 2b). Between 0 and 150 km offset, the amplitudes are close to 0 while at approximately 150 km offset there is an overall increase in the amplitudes for both shot gathers. The amplitude pattern for shot # 4 also starts at 150 km offset, with a small increase in the amplitudes. Ray path diagrams by Carbonell et al., [1996] indicated that these two shot gathers (#'s 1 and 4) sampled the Moho beneath the Magnitogorsk volcanic arc. Therefore, the amplitude pattern at 150-160 km offset can be interpreted as the increase in amplitude expected at critical distances. A crustal thickness of 51 - 55 km beneath the southern Urals is estimated assuming an upper mantle velocity of 8.0-8.1 km/s, an average crustal velocity of 6.5-6.6 km/s (taken from Carbonell et al., [1996]), and a critical distance of between 150-160 km.

The wide-angle stacked image reveals a well constrained Moho across the southern Urals centered at approximately 15 ± 1 s. (Fig. 3a). Error estimates of t_0 of ± 1 s and υ_0 of ± 0.2 km/s result in TWT variations of 0.7s. The depth converted stack for an average velocity of 6.6 (Fig. 3b) displays a maximum crustal thickness of approximately 53 ± 2 kms located beneath the Magnitogorsk arc, and shallowing toward the west and east. This estimate nearly overlaps with the 55-58 km depth reported previously [Carbonell et al., 1996]. The relatively small difference is probably a result of using a constant average velocity in equation (1). The Moho is not a simple, smoothly curving feature as envisioned by Berzin et al. [1996], but rather undulates, and displays a rough topography with up to 1 s of relief (Fig. 3a). A composite section of the travel time picks of the wide-angle PmP phase from Fig 3a, superimposed on the normal incidence explosive CMP stacked section of Steer et al. [1998], reveals only a moderate increase in the crustal thickness (from 40-45 km at the edges of the transect [Steer et al., 1998]) reaching 50-53 km beneath the central part of the orogen (Fig. 3c).

The processing scheme used here can also be used to provide stacks for selected offsets. By choosing the traces around the critical distances (~150 - 160 km), the theoretically highest amplitudes can be selected. Although the Moho appears to consist of a series of arcuate events (Fig. 3d), this is probably not a direct image of the real structure since this technique images the Moho from the critical distance and the arcuate events are, therefore, most likely far offset diffractions resulting from a rough Moho. These diffractions, however, provide strong evidence for the topographic relief of the Moho in this area. Rough Moho topography has been proposed for other areas [Larkin et al., 1997]. This complexity of the Moho beneath the Magnitogorsk arc (an area that coincides with the Late Devonian and Late Carboniferous - Early Triassic subduction zones) suggests that is has undergone a significant re-equilibrium process, but still retains important differences relative to the Moho beneath the EEC or the accreted terranes to the east.

This difference in Moho character is also reflected in the variable nature of the PmP wavelet along the transect. Beneath the former EEC, PmP is a relatively short, simple wavelet comparable to the first arrival (e.g., the source signal) and is indicative of a relatively simple crust-mantle transition that can be easily simulated by a step in the velocity-depth function. Beneath the Magnitogorsk arc, however, the wavelet of the PmP phase is relatively simple along its western margin, becoming more complex eastward (e.g., CMP 700 - 1000) and the reflectivity becomes distributed along an approximately 2 s thick zone consisting of several prominent bands. East of the Magnitogorsk arc, the PmP phase is marked by a high amplitude multicyclic wavelet. To conclude, in contrast to the high frequency normal incidence reflection data (e.g., Steer et al., 1998), the low frequency wide-angle data provides a complete Moho image across the southern Urals.

Acknowledgements. This research was partly funded by the TMR network URO (ERBFMRXCT960009). Funding for URSEIS-95 by CICYT, Spain (AMB 95-09987E, UE95-0026); ROSCOMNEDRA (Russia); DEKORP 2000 (grant 03GT94101) and GFZ Potsdam, The Continental Dynamics Program (NSF grant EAR-9418251), Cornell, USA, and by INTAS grant 94-1857. Two anonymous reviewers and A. Levander are thanked for their comments.

References

Berzin, R., O. Oncken, J.H. Knapp, A. Perez-Estaun, T. Hismatulin, N. Yunusov, and A. Lipilin, Orogenic evolution of the Ural Mountains: Results from an integrated seismic experiment, *Science, 274*, 220-221, 1996.

Brown, D., J. Alvarez-Marron, A. Perez-Estaun, Y. Gorozhanina, V. Baryshev, and V. Puchkov, Geometric and kinematic evolution of the foreland thrust and fold belt in the southern Urals, *Tectonics, 16*, 551-562, 1997.

Brown, D., C. Juhlin, J. Alvarez-Marron, A. Perez-Estaun, and A. Oslianski, Crustal-scale structure and evolution of an arc-continent collision zone in the southern Urals, Russia, *Tectonics*, 17, 158-170, 1998.

Carbonell, R., A. Perez-Estaún, J. Gallart, J. Diaz, S. Kashubin, J. Mechie, R. Stadtlander, A. Schulze, J.H. Knapp, and A. Morozov, A crustal root beneath the Urals: Wide-angle seismic evidence, *Science, 274*, 222-224, 1996.

Druzhinin, V.S., S.N. Kashubin, S.V. Avtoneev, S.V. Avtoneyev, and V.M. Rybalka, New data on deep structure of the southern Urals according to results of investigations on the Troitsk DSS profile, *Sov. Geol. Geophys., Engl. Transl.*, 29, 79-82, 1992.

Echtler, H.P., M. Stiller, F. Steinhoff, C.M. Krawczyk, A. Suleimanov, V. Spiridonov, J. Knapp, Y. Menshikov, J. Alvarez-Marron, and N. Yunusov, Preserved collisional crustal architecture of the southern Urals - Vibroseis CMP-profiling, *Science, 274*, 224-226, 1996.

Fershtater, G.B., P. Montero, N.S. Borodian, E.V. Pushkarev, V.N Smirnov, and F. Bea, Uralian magmatism: an overview. *Tectonophyics*, 276, 87-102, 1997.

Hajnal, Z., S. Lucas, D. White, J. Lewry, S. Bezdan, M.R. Stauffer, and M.D. Thomas, Seismic reflection images of high-angle faults and linked detachments in the Trans-Hudson Orogen, *Tectonics*, 15, 427-439, 1996.

Juhlin, C., J.H. Knapp, S. Kashubin, and M. Bliznetsov, Crustal evolution of the Middle Urals based on seismic reflection and refraction data, *Tectonophysics, 264*, 21-34, 1996.

Khain, V., 1985. Geology of the USSR. Schweizerbart'scheBorntanger, Stuttgart, 272 pp.

Knapp, J.H., D.N. Steer, L.D. Brown, R. Berzin, A. Suleimanov, M. Stiller, E. Lüschen, D. Brown, R. Bulgakov, and A.V. Rybalka, A lithosphere-scale image of the Southern Urals from explosion-source seismic reflection profiling in URSEIS '95, *Science,* 274, 226-228, 1996.

Larkin, S., A. Levander, T.J., Henstock, and S. Pulammanappallil, Is the Moho flat? Seismic evidence for a rough crust-mantle interface beneath the northen Basin and Range, *Geology*, 25, 451-454, 1997.

Puchkov, V.N., Structure and geodynamics of the Uralian orogen, in *Orogeny Through Time*, edited by J.-P. Burg and M. Ford, *Geol. Soc. Spec. Publ. 121*, 201-236, 1997.

Steer, D.N., J.H. Knapp, L.D. Brown, H.P. Echtler, D.L. Brown, and R. Berzin, Deep structure of the continental lithosphere in an unextended orogen: An explosive-source seismic refelction profiles in the Urals (Urals Seismic Experiment and Integrated Studies (URSEIS 1995)), *Tectonics*, 17, 143-157, 1998.

Thouvenot, F., S.N. Kashubin, G. Poupinet, V.V. Makovski, T.V. Kashubina, Ph. Matte, and L. Jenatton, The roots of the Urals: evidence from wide-angle reflection seismics, *Tectonophysics*, 250, 1-13, 1995.

Valasek, P., St. Muller, W. Frei, and K. Holliger, Results of NFP20 seismic reflection profiling along the Alpine section of the European Geotraverse (EGT), *Geophys. J. Int.*, 105, 85-102, 1991.

Valasek, P., and St. Muller, A 3D tectonic model of the Central Alps based on integrated interpretation of seismic refraction and NFP20 reflection data. In V. A. Pfiffner, P. Lehner, P. Heitzmann, St. Muller, A. Steck eds. Deep structure of the Alps, Results of NRP20. Birkhäuse Verlag Basel, 305-325, 1997.

Zonenshain, L.P., V.G. Korinevsky, V.G. Kazmin, D.M. Pechersky, V.V. Khain, and V.V. Mateveenkov, Plate tectonic model of the south Urals development, *Tectonophysics*, 109, 95-135, 1984.

Zonenshain, L.P., M.I. Kuzmin, and L.M. Natapov, Uralian Foldbelt, in *Geology of the USSR: A Plate-Tectonic Synthesis*, Geodyn. Ser., vol. 21, edited by B.M. Page, pp. 27-54, AGU, Washington, D. C., 1990.

R. Carbonell, J. Gallart, D. Brown, Dept. Gephysics, Inst. of Earth Sciences, CSIC-Barcelona, 08028 Barcelona, Spain. (e-mail: rcarbo@ija.csic.es)

D. Lecerf, M. Itzen, Gophysical Institute, Kerlsruhe University, Karlsruhe, Germany.

(Received April 30, 1998; revised July 27, 1998; accepted September 23, 1998.)